Removal of methylene blue from aqueous solution by natural phosphate

KAMEL RIDA*, BILAL CHEMMAL, ALI BOUKHEMKHEM
Laboratoire d'Interaction Matériaux Environnement (LIME), Université de Jijel, Algérie

This study investigated the potential use of natural phosphate (Djebel Onk – Tebessa-Algeria) as alternative adsorbents for removal of methylene blue from wastewater. The adsorbent was characterized by powder X-ray diffraction, FT-IR spectroscopy, BET surface area and scanning electron microscopy (SEM). The effects of initial dye concentration, contact time, adsorbent dose, stirring speed, pH, salt concentration and temperature were studied in batch mode. The experimental isotherms were analyzed using Langmuir and Freundlich isotherm equations. Thermodynamic parameters such as, ΔG, ΔH, ΔS and the activation energy were calculated. The kinetic studies indicated that the adsorption process followed the pseudo second-order mode, suggesting that the adsorption might be a chemisorption process. The present study implied that natural phosphate was a promising candidate for the removal of dye molecules from aqueous solution.

(Received April 17, 2013; accepted June 12, 2013)

Keywords: Methylene blue, Natural phosphate, Adsorption, Isotherms, Kinetics

1. Introduction

Organic effluents from industries such as the automotive industry, tannery, paper and especially the textile sector often have a significant colouring related to the pollutant load. The complexity and low biodegradability of such pollutants makes biological treatments difficult to apply, while they constitute an important source of degradation of the environment and pose a health concern because most of such dyes are toxic.

In this context, several methods have been used, among other coagulation/flocculation [1], adsorption on activated carbon and, most recently, electrocoagulation [2], which can be effective, but in most cases, very expensive. The research in this field is then directed to methods of treatment using natural materials such as clays (sepiolite, zeolithe, montmorillonite, smectite, bentonite, alunite and perlite) agricultural materials (sawdust, agricultural waste, ...) and some industrial discharges because of their availability and low costs [3, 4].

Natural phosphate (NP) has been used as phosphate fertilizers for many years, especially in acid soils. Fluorapatite is the principal constituent of igneous phosphate rock. The structure of hydroxyapatite is similar to that of fluorapatite, for OH^- can occupy the sites of F^- on the 6-flod axis. The apatites in sedimentary phosphate are poorly crystallized, and their compositions differ considerably from those of pure apatite. Their chemical reactivity and thermal stability vary widely as a result, depending on the degree of isomorphic substitution of carbonate for phosphate in the fluorapatite crystal lattice [5].

From our part, we are interested in the natural phosphate, an abundant material; in turn, it can be widely used the textile industry to eliminate the cationic dye methylene blue. Algerian Natural Phosphates are primarily sedimentary. Phosphates have physicochemical and textural characteristics which can be most interesting for mentioned process. They are able to establish connections with organic molecules of different sizes. In this sense, calcium phosphates are very much studied in the removal of heavy metal ions [6], fluoride [7], nitrobenzene [8] and protein [9]. Barka et al. [10] have showed that both materials were effective to remove dyes.

The objective of this study was to test the possibility of using the natural phosphate (NP) for the removal of methylene blue (MB) from aqueous solutions. The second objective was to establish the ability of two isotherms models; the Langmuir and the Freundlich adsorption isotherms, to model the equilibrium adsorption data. Finally, kinetic studies have been also conducted to determine the rate of MB adsorption on NP and to suggest probable mechanism of the process.

2. Materials and methods

2.1. Adsorbate

The basic dye used in this study was methylene blue (MB) purchased from Sigma-Aldrich. MB has a molecular weight of 373.9 g/mol, which corresponds to methylene blue hydrochloride with three groups of water. The maximum absorption wavelength of this dye is 668 nm. The MB was chosen in this study because it was used in numerous adsorption studies to evaluate the capacity of different adsorbents, thus placing the results of the current study in perspective. The solutions were prepared by dissolving the required amount of dye in distilled water.

2.2. Preparation of the adsorbent

The mineral phosphate rock used in this study was from the mine of Djebel Onk (East of Algeria). It was washed with distilled water and dried at 103°C for 24 h to remove moisture. The fraction between 100 and 400 µm grain size which contains phosphate phases was retained and ground to obtain a homogenous sample having a grain size below 125 µm. No other chemical or physical treatments were applied prior to adsorption experiments. Table 1 shows the chemical analysis of the major constituents of natural phosphate (NP).

Table 1. Chemical composition of NP sample.

Analysis	P_2O_5	CaO	MgO	CO_2	SiO_2	Fe_2O_3	Al_2O_3	SO_3	K_2O	Na_2O	F	Cl	Organic matter	Moisture
%	29.04	49.89	1.15	7.18	2.14	0.31	0.39	3.22	0.15	1.21	3.68	0.04	0.26	0.76

2.3. Characterization of the adsorbent

The X-ray diffraction patterns of natural phosphate were measured using a Bruker diffractometer (D8 Advance) with Ni-filtered copper radiation (Kα=1.5406 Å) and 2θ range of 10–80°.

Fourier Transform Infrared (FTIR) analysis was applied to determine the surface functional groups, by using FTIR spectroscope (FTIR- 8400 S Shimadzu), where the spectra were recorded from 4500 to 400 cm^{-1} and the samples were prepared as KBr pellets under high pressure.

Textural characterization of the activated carbon was done by using N_2 adsorption–desorption at 77K in a Micromeritics ASAP2010 apparatus. The specific surface area was determined by the BET isotherm equation, and the total pore volume (V_{tot}) was calculated by the adsorption data at $P/P_0 = 0.995$. Prior to the measurements, the samples were outgassed at 140°C under nitrogen for at least 3 h.

The point of zero charge was determined according to the method described by Ferro-Garcia et al. [11].

The morphology of the NP was analyzed by scanning electron microscopy (SEM, Philips XL30).

2.4. Adsorption studies

Batch experiments are carried out using a 2 L capacity glass beaker at ambient temperature. Stock solution of BM of concentration 1000 mg/L is prepared by dissolving an accurately weighed quantity (1.0 g) of solid dye in 1 L of deionized water (pH is 6.9). Experimental solutions of desired concentrations are obtained by successive dilution of the stock solution. Standard technique is used to determine the dye concentration using UV–vis spectrophotometer. Initial dye concentrations are varied from 1.6 to 16 mg/L. For studying the effect of solution pH on dye adsorption, experiments at different pH (varying from 2. to 11) have been conducted for initial dye concentration of 3.2 mg/L. To observe the effect of adsorbent dose on dye adsorption, different amounts of adsorbent (varying from 25 to 250 mg/L) are used initial dye concentration, 3.2 mg/L. To observe the effect of temperature on dye adsorption, experiments are carried out at three different temperatures (21, 40 and 50°C), where all other variables remain unchanged. A common adsorbent dose of 1 g/L, stirring speed of 800rpm and pH 7 is used for all the above experiments. Different agitation speeds of 250 - 800 rpm are used for observing the effect of turbulence on the dye adsorption.

The amount of dye adsorbed per unit weight of phosphate at time t, q_t (mg/g) and percentage dye removal efficiency, R are calculated as follows:

$$q_t = \frac{(C_0 - C_t)}{M} V \quad (1)$$

$$R = \frac{C_0 - C_t}{C_0} \times 100 \quad (2)$$

where C_0 is the initial dye concentration (mg/L), C_t is the concentration of dye at any time t, V is the volume of solution (L) and M is the mass of phosphate (g).

In order to study the adsorption isotherm, 0.025 g of NP is kept in contact with 25mL dye solution of different concentrations for 2 to 3 h (to get confirm that the equilibrium has been reached) with constant shaking at ambient temperature. After the equilibrium, the solution attains equilibrium and the amount of dye adsorbed (mg/g) on the surface of the adsorbent is determined by the difference of the two concentrations.

3. Results and discussions

3.1. Characterization of adsorbent

The XRD patterns of the fine fraction of NP used in the present study is shown in Fig. 1. The mineralogical composition of the natural phosphate was reported in Bezzi et al. [12]. Carbonated fluoroapatite was identified as a major component of this NP. Dolomite, calcite and quartz are the other associated gangue minerals.

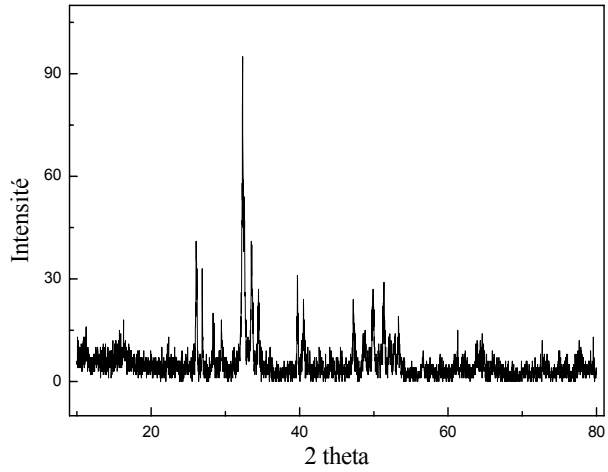

Fig. 1. XRD pattern of natural phosphate NP.

In the FTIR spectrum of NP (Fig. 2) there is strong evidence on the presence of some functional groups. Broad band around 3400 cm^{-1} was due to stretching vibration of O-H bond in hydroxyl groups. The peak located at 1736 cm^{-1} was characteristic of carbonyl group stretching. The peak at 1603 cm^{-1} was due to bending vibration of O-H groups. The bands of phosphate at around 1050 cm^{-1} appear as a single intense band. Another distinct phosphate band of bending mode appears around 660-520 cm^{-1}.

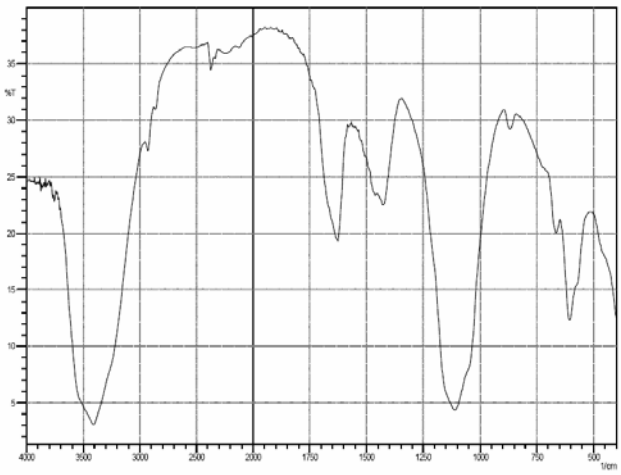

Fig. 2. IR spectrum of natural phosphate NP.

The BET surface area was found to be 35 m^2/g and the total pore volume 0.075 mL/g. The distribution of pore size reveals that the dominant pore size is 14 nm. The pore size distribution of NP makes it suitable for adsorbing dye molecules like MB because the monomers of MB molecule have a minimum molecular cross-section of about 0.8 nm and cannot enter the pores with diameter less than 1.25 nm [13].

The textural structure examination of NP particles can be observed from the SEM photographs at 430× magnification (Fig. 3). This figure reveals that the NP particles were mostly irregular in shape and seem to be nonporous. It is noticed that the particle size distribution is not continuous, relatively large particles are mixed with much finer size ones.

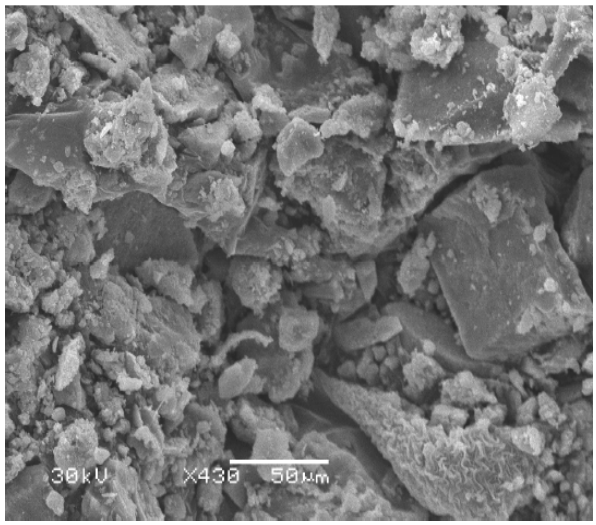

Fig. 3. SEM image of natural phosphate NP.

3.2. Adsorption studies

3.2.1. Effect of contact time and initial dye concentration

The kinetics of adsorption of MB at different initial concentration is shown in Fig. 4. It is found that, as the initial concentration increases, the equilibrium time and the amount of dye adsorbed per gram amount of adsorbent increase. The rapid adsorption of dye takes place within 5 min for both the dyes, and then the adsorption becomes slower and almost reached equilibrium within 30 min.

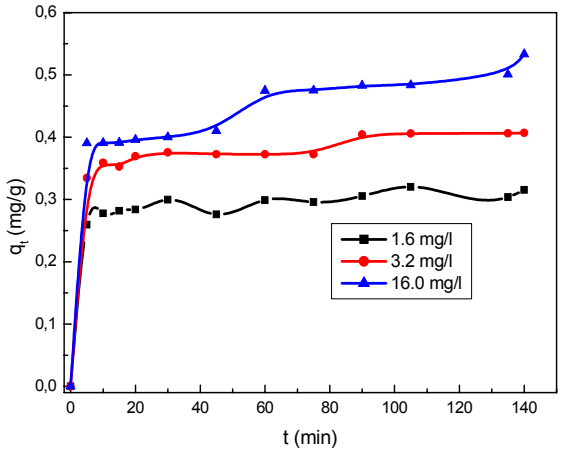

Fig. 4. Effect of contact time and initial concentration of MB on the adsorption.

For the initial concentration up to 1.6 mg/L, more than 12% removal has been observed for MB. For 16 mg/L, the removal of MB was 37%.

3.2.2. Effect of adsorbent dosage

The results concerning the effect of adsorbent dosage are shown in Fig. 5. As indicated, 42% of BM was removed at the initial quantity of 0.025g of NP. The removal of dye increased with increasing solid quantity up to 0.15 g and reached to 85% for MB at this quantity. However it is observed that after a dosage of 0.15 g of NP, there was no significant change in the percentage removal of dye. This may be due of the saturation of active sites at higher dosage [14].

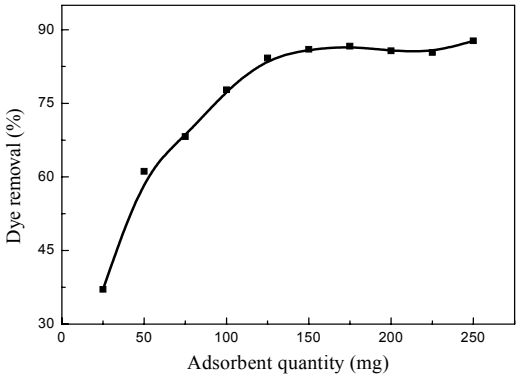

Fig. 5. Effect of adsorbent quantity on the adsorption of MB.

3.2.3. Effect of stirring speed

The effect of stirring speed on the removal of MB on phosphate was investigated at different stirring speeds such as 250-850 rpm at 21°C as seen from Table 2. The difference of the adsorption rate was insignificant as the stirring speed increased; the dye removal does not exceed 50%.

Table 2. Effect of stirring speed.

Stirring speed (rpm)	250	350	500	650	800
Dye removal (%)	44.72	39.49	47.68	41.22	45.35

3.3.4. Effect of ionic strength

The effect of salt concentration (ionic strength) on the removal percentage of MB by natural phosphate is analyzed along the KCl amount range from 10 to 25 mg. Sorption kinetics are carried out for lead initial concentration of 3.2 mg/L, solution volume of 1 L, and a sorbent mass of 1 g. The obtained results are shown in Fig. 6. Higher MB removal takes place when the ionic strength of the solution is increased from 10 to 25 mg. According to the electrostatic double layer (EDL) theory [15], the electrostatic double layer (EDL) of the NP is compressed when ionic strength of the solution is increased.

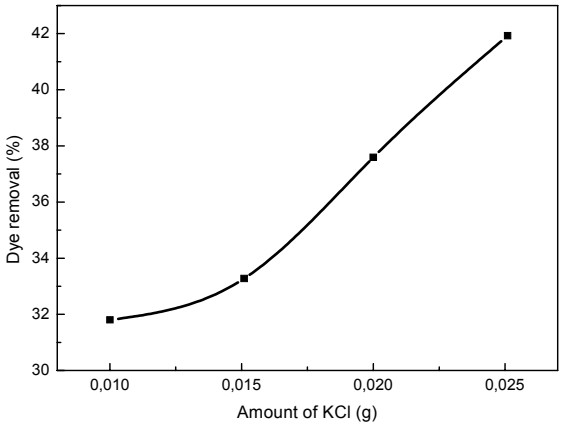

Fig. 6. Effect of KCl concentration on the removal capability.

3.2.5. Effect of solution pH on dye adsorption

In this work, the effect of pH on the MB adsorption onto NP was studied while the initial dye concentration and amount of NP and temperature were fixed at 3.2 mg/L, 0.025g and 21°C, respectively. The effect of pH on the adsorption of MB by the NP is presented in Fig. 7. The effect of pH on adsorption of dye was studied within pH range of 2–11. The solution pH would affect both aqueous chemistry and surface bindingsites of the adsorbent. MB is a very weak base and reacts only in the solutions of strong acids to yield low amounts of protonated cations [16], therefore it is safe to assume that MB is a positively charged, unprotonated-cation, throught the pH range investigated (2-11). The point of zero charge of NP was found to be at a pH value 7,6.

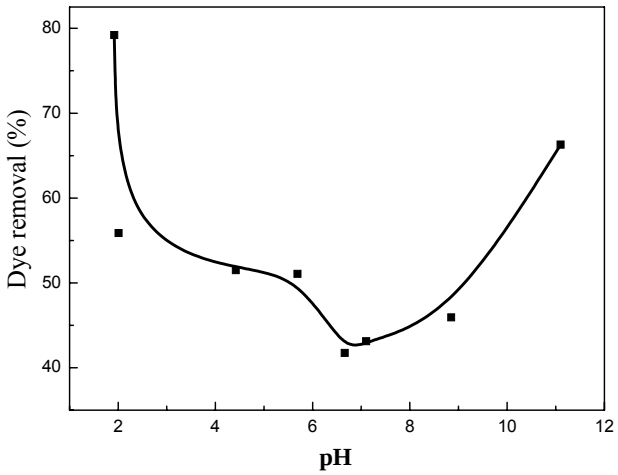

Fig. 7. Effect of pH on the adsorption % of methylene blue.

The equilibrium sorption capacity was minimum at pH 6.5-8 (45%) and increased up to pH 2 (80%). At higher solution pH, the NP becomes negatively charged, which enhances the positively charged dye cations through electrostatic forces of attraction and increased sorption capacity to 70%. A similar result of pH effect was also reported for the adsorption of MB onto jute fiber carbon [17] and Bentonite [18]. A pure electrostatic interaction between the negative charge of the NP and the positive charge of the dye cannot be the only mechanism of adsorption. A different type of interaction should account for the adsorption process because high amount of dye is adsorbed at pH values lower than the PZC. Moreover, an increase in the adsorption capacity occurs three pH units above the PZC. These facts point to the existence of hydrophobic interactions which have been suggested by different authors to have a role on the interaction of methylene blue with different kind of surfaces [19-23].

3.3. Sorption kinetic study

In an attempt to present the kinetic equation representing adsorption of MB onto NP, three kinds of kinetic models were used to test the experimental data. These are Lagergren-first-order equation (Eq. (3)), second-order equation (Eq. (4)), and intraparticle diffusion model (Eq. (5)).

$$\ln(q_e - q_t) = \ln q_e - k_1 t \quad (3)$$

$$1/q_t = 1/k_2 q_e^2 + t/q_e \quad (4)$$

$$q_t = k_{id} t^{0.5} + I \quad (5)$$

where q_t (mg/L) is the amount of adsorption time t (min), q_e is the amount of adsorption at equilibrium (mg/g), k_1, the rate constant of the first-order equation (min^{-1}), k_2 (g/mg.min) is the rate constant of the second-order equation; and k_{id} (mg/g/min) is the rate constant of intraparticle diffusion. Values of I give information about the thickness of the boundary layer, i.e. the larger intercept the greater is the boundary layer effect.

Table 3 lists the results of the kinetic parameters calculated using the pseudo-first-order and pseudo-second-order models. The curve fitting plots of $ln\ (q_e-q_t)$ versus t does not show good results for the sorption (figure not shown) because the coefficient of determination for this model is low (R^2 = 0.44 – 0.77).

Table 3. Kinetic parameters for adsorption of methylene blue on natural phosphate.

C_0 (mg/l)	$q_{e,exp}$ (mg/g)	Pseudo first order			Pseudo second order			Intraparticule diffusion		
		k_1 (min^{-1})	$q_{e.cal}$ (mg/g)	R^2	k_2 ($g.mg^{-1}.min^{-1}$)	$q_{e.cal}$ (mg/g)	R^2	k_{id} ($mg./g.min^{-1}$)	I (mg/g)	R^2
1.6	0.32	0.09	0.05	0.492	1.88	0.31	0.997	0.005	0.26	0.862
3.2	0.41	0.25	0.04	0.772	0.02	0.41	0.989	0.007	0.33	0.928
16	0.53	0.23	0.02	0.491	0.24	0.52	0.981	0.015	0.34	0.954

The plots of t/q_t versus t give a straight line as seen from Fig. 8. The correlation coefficients of pseudo-second-order were closer to unity and calculated q_e values computed from pseudo-second order equation showed good agreement with experimental values. This supports the assumption of the model that the adsorption is due to chemisorption [24].

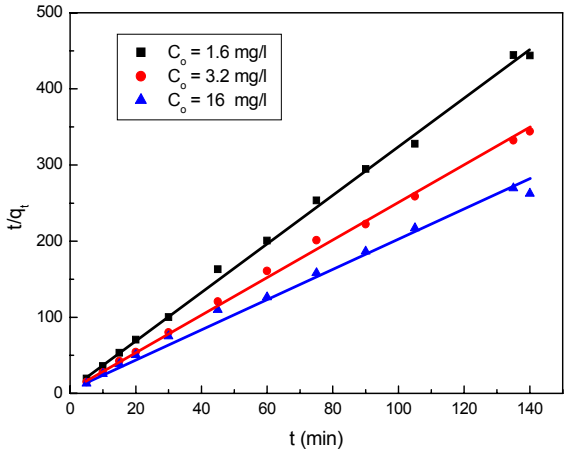

Fig. 8. Pseudo-second order kinetic plots for the adsorption of MB on NP.

To identify the importance of diffusion in the adsorption process, the parameters calculated using the plots of q_t versus $t^{0.5}$ are presented in Table 3. Fig. 9 showed the involvement to two steps in the adsorption process, the first one representing adsorption of dyes on the surface of adsorbent and the second one describing the diffusion of dyes to the adsorption site. Surface adsorption mechanism was dominant in first 5 min of contact time thereafter diffusion became a rate-limiting process. The values of $I \neq 0$, indicates that the intraparticle diffusion was involved in the adsorption process, but was not the only rate controlling step. Rates of diffusion were higher at initial concentration of MB, resulting in high adsorption capacity. From the obtained results it can be concluded that both surface adsorption and intraparticle diffusion mechanism was followed in all cases for the adsorption.

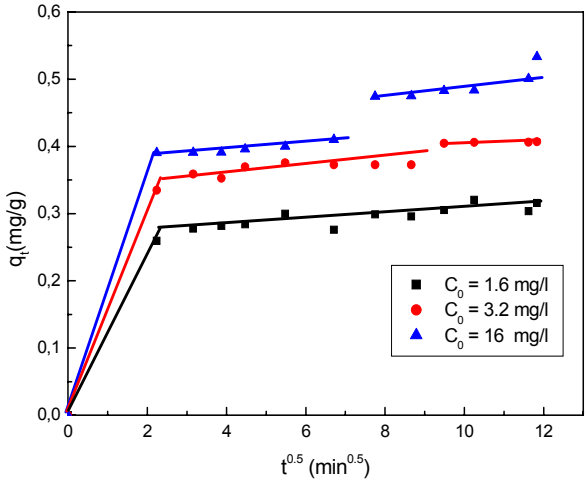

Fig. 9. Intraparticle plots for the adsorption of MB on NP.

3.4. Calculation of thermodynamic parameters

3.4.1. Calculation of the change free energy change (ΔG)

To estimate the effect of temperature on the adsorption of MB onto NP, the free energy change (ΔG), enthalpy change (ΔH), and entropy change (ΔS) were determined by the Erring equation [25].

$$\ln\left(\frac{k_2}{T}\right) = \ln\left(\frac{k_B}{h_p}\right) + \frac{\Delta S}{R} - \frac{\Delta H}{R\ T} \qquad (6)$$

where k_B and h_p are Boltzmann's (1.3807×10^{-23} J K^{-1}) and Planck's (6.6261×10^{-34} J s) constants, respectively., and k_2 the rate constants of the pseudo-second-order model. Gibbs energy may be written in terms of entropy and enthalpy:

$$\Delta G = \Delta H - T\Delta S \qquad (7)$$

Values of the standard Gibbs free energy change for the adsorption process obtained from Eq. (7) were listed in Table 4.

The negative ΔG value of MB adsorption onto NP was due to the fact that the adsorption processes were spontaneous with a high preference of MB onto NP and the negative value of ΔG° decreases with an increase in temperature, indicating that the spontaneous nature of adsorption of MB was inversely proportional to the temperature and higher temperature favored the adsorption.

Table 4. Thermodynamic parameters for the adsorption of MB on NP.

ΔH (J.mol^{-1})	ΔS (J.mol^{-1}K^{-1})	ΔG (Kj.mol^{-1}) 294 K	303 K	313 K
0.28	175.51	-51.60	-53.18	-54.93

The standard enthalpy and entropy changes of adsorption determined from Eq. (6) were 0.29 k.mol^{-1} and 175.51 J.mol^{-1}.K^{-1}, respectively. The positive value of ΔH confirmed the endothermic character of the adsorption on MB/NP system whereas the positive ΔS values confirmed the increased randomness at the solid–solute interface during adsorption. The low value of ΔS° also indicated that no remarkable change of entropy occurs.

3.4.2. Estimation of activation energy

Fig. 10 shows a linear relationship between the logarithm of the rate constant and the reciprocal of temperature. The second order rate constant is expressed as a function of temperature using the Arrhenius equation [26]:

$$k_2 = k_0 \exp(-E / RT) \qquad (8)$$

where k_0 is the temperature independent factor (g.mg^{-1}.min^{-1}); E the activation energy of sorption (kJ.mol^{-1}); R the gas constant (8.314 J.mol^{-1}.K^{-1}), and T is the solution temperature (K).

From this equation, the rate constant of sorption, k_0, is 8.23×10^{-4} g.mg^{-1}.min^{-1} and the activation energy of sorption E is 2,37 kJ.mol^{-1}. The low value of the energy of activation suggests the existence of a physical adsorption [27]. Therefore, the affinity of methylene blue for the NP may be ascribed to Van Der Waals forces or hydrogen

bonds between the dye and the surface of the particles NP. However, the real process is much more complex.

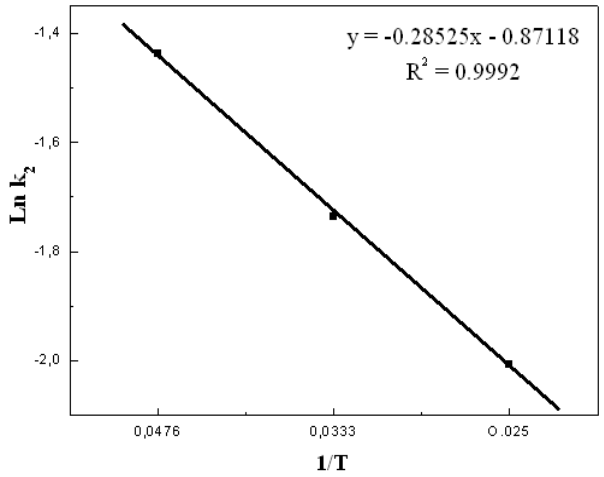

Fig. 10. Arrhenius plot for the adsorption of MB on phosphate NP.

3.5. Equilibrium isotherms

In the present investigation the equilibrium data were analyzed using the Langmuir and Freundlich isotherm expression given by Eqs. (9) and (10), respectively:

$$\frac{q_e}{q_m} = \frac{K_L.C_e}{(1 + K_L.C_e)} \tag{9}$$

$$q_e = K_F C_e^{1/n} \tag{10}$$

where *Ce* is the equilibrium concentration (mg /L), q_e is the amount of dye adsorbed at equilibrium (mg/g), and q_m and K_L are Langmuir constants related to adsorption capacity and energy of adsorption, respectively. K_F and n are the Freundlich constants, which are indicators of adsorption capacity and adsorption intensity, respectively [28].

Fig. 11-12 shows the fitted equilibrium data in Freundlich and Langmuir isotherms. The fitting results, i.e. isotherm parameters and the coefficients of determination, R^2, are shown in Table 5. It can be seen in Fig. 12 that Langmuir isotherm fits the data better than Freundlich isotherm (Fig. 13). This is also indicated by the high value of R^2 in case of Langmuir (0.9785) compared to Freundlich (0.9464) and this indicates that the adsorption of MB on NP takes place as monolayer adsorption on a surface that is homogenous in adsorption affinity.

Table 5. Isotherm parameters for the adsorption of MB on NP.

Langmuir isotherm parameters			Freundlich isotherm parameters		
q_m (mg/g)	K_L (l/mg)	R^2	K_F (mg/l)	n_F (l/g)	R^2
44.39	0.177	0.9785	0,577	1.076	0,9464

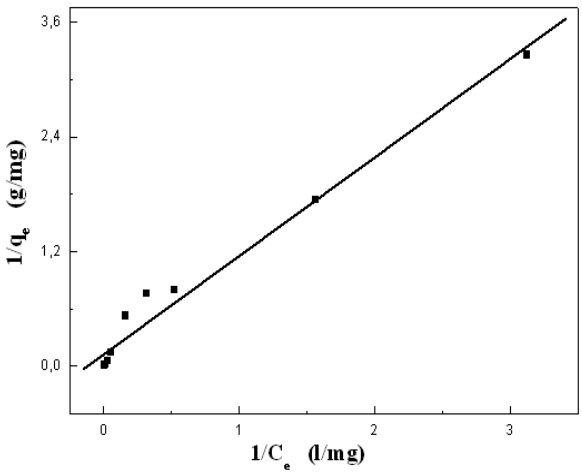

Fig. 11. The Langmuir plots for the adsorption of MB on NP.

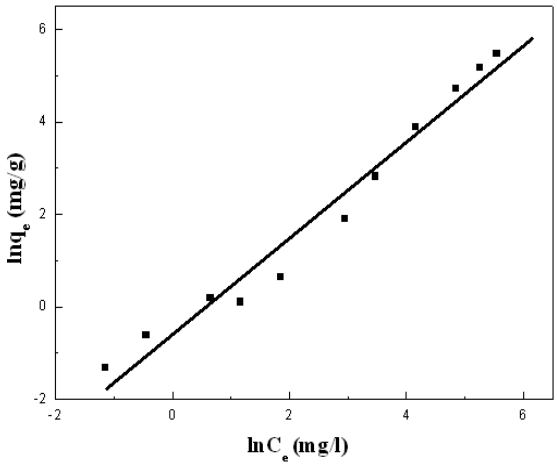

Fig. 12. The Freundlich plots for the adsorption of MB on NP.

The NP adsorbent used in this work had a relatively large MB adsorption capacity (44.39mg/g) compared to some other adsorbents reported in the literature, such as bentonite clay (7.72 mg/g) [29], arundo donax root carbon (8.70 mg/g) [30]. This indicates that NP is effective in removing MB from aqueous solutions.

4. Conclusions

The study presented revealed that natural phosphate (NP) can be used as a low-cost adsorbent for removing cationic dyes. The adsorption was highly dependent on various operating parameters, like: contact time, pH, initial dye concentration, ionic strength. The adsorption kinetics was very well described by the pseudo-second-order kinetic model. The equilibrium of adsorption of MB onto natural phosphate was adequately described by the Langmuir and Freundlich isotherm models. Thermodynamic studies indicated that the dye adsorption process onto phosphate (NP) is physical, spontaneous and endothermic in nature

Acknowledgements

This work was financed by Ministère de l'enseignement supérieur et de la recherché scientifique of Algeria. Thanks are due to the Instituto de Catálisis y Petroleoquímica (CSIC, Spain) Unidad de Apoyo staff for the performance of characterization experiments (XRD, adsorption isotherms) and to Prof. Arturo Martínez-Arias for the revision of the manuscript.

References

[1] S. Kacha, M. S. Ouali, S. Elmalah, Rev. Sci. Eau. **2,** 233 (1997).
[2] S. Shim, Y. Kim, S-K.Jung, K-H. Suh, S-G.Kang, S-K. Jeong, H-G. Kim, Korean J. Chem.Eng. **4**, 806 (2004).
[3] S. Tahiri, A. Messaoudi, A. Alibizane, M. Azzi, M. Bouhria, S. Alami Younsi, J. Mabrour, Water Qual. Res. **38**, 393 (2003).
[4] S. Albariji, M. Alamine, H. Kabli, A. Lacherai, A. El-Bourine, C. R. Chimie. **9**, 1314 (2006).
[5] M. Mouflih, A. Aklil, N. Jahroud, M. Gourai, S. Sebti, Hydromatallurgy. **81**, 219 (2006).
[6] Y. Feng, I. L. Gong, G. M. Zeng, Q. Y. Niu, H. Y. Zhang, C. G. Niu, J. H. Deng, M. Yan, Chem. Eng. J. **162**, 487 (2010).
[7] G. E. J. Poinern, M. K. Ghosh, Y. J. Ng, T. B. Issa, S. Anand, P. Singh, J. Hazard. Mater. **185**, 29 (2011).
[8] W. Wei, R. Sun, J. Cui, Z. Wei, Desalination. **263**, 89 (2010).
[9] Z. Yang, C. Zhang, Appl. Sur. Sci. **255**, 4569 (2009).
[10] N. Barka, S. Qourzal, A. Assabbane, A. Nounah, Y. Ait-Ichou, J. Saudi. Chem. Soci. **15**, 263 (2011).
[11] M. A. Ferro-Garcia, J. Rivera-Utrilla, I. Bantista-Toledd, A. C. Moreno-Castilla, Langmuir. **14**, 1880 (1998).
[12] N. Bezzi, D. MErabet, N. Benabdeslem, H. Arkoub, Annales de Chimie. **26**, 5 (2001).
[13] H. Valdes, M. Sanchez-Polo, J. Rivera-Utrilla, C. A. Zaror, Langmuir. **18**, 2111 (2002).
[14] I. D. Mall, V. C. Srivastava, N. K Agarwal, I. M Mishra, Chemosphere. **61**, 492 (2005).
[15] J. P. Chen, M. Lin, Carbon. **39**, 1491 (2001).
[16] A. Czímerová, L. Jankovi, J. Bujdák, J. Colloid. Interface. Sci. **274**, 126 (2004).
[17] S. Senthilkumaar, P. R. Varadarajan, K. Porkodi, C. V. Subbhuraam, J. Colloid. Interface Sci. 284, **78** (2005).
[18] C. Bilgiç, J. Colloid. Interface. Sci. **281**, 33 (2005).
[19] R. Guy, D. Narine, Can. J. Chem. **58**, 555 (1980).
[20] K. Imamura, E. Ikeda, T. Nagayasu, T. Sakiyama, K. Nakanishi, J. Colloid. Interface. Sci. **245**, 50 (2002).
[21] N. Mchedlov-Petrossyan, V. Klochkov, G. Andrievsky, A. Ishchenko, Chem. Phys. Lett. **341**, 237 (2001).
[22] D. Palit, S. Moulik, Colloid. J. **65**, 350 (2003).
[23] E. Rubin, P. Rodriguez, R. Herrero, J. Cremades, I. Barbara, M. Sastre de Vicente, J Chem. Tech. Biotechnol.. **80**, 291 (2003).
[24] E Bulut, M.Ozacar, I. A Sengn, Micropor. Mesopor. Mater. **115**, 234 (2008).
[25] K. L. Laidler, J. H. Meiser, "Physical Chemistry ", Houghton Mifflin, New York.
[26] M. Dogan, M. Alkan, Chemosphere. **50**, 517 (2003).
[27] H. Nollet, M. Roels, P. Lutgen, P. Van der Meeren, W. Verstraete, Chemosphere. **53**, 655 (2003).
[28] K. V. Kumar, V. Ramamurth, S. Sivanesan, Dyes Pigments. **69**, 102 (2006).
[29] S. S. Tahir, N. Rauf, Chemosphere. **63**, 1842 (2006).
[30] J. Zhang, Y. Li, C. Zhang, Y. Jing, J. Hazard. Mater. **150**, 774 (2007).

*Corresponding author: rida_kamel2001@yahoo.fr